# Raman Scattering by Optical Phonons
# in a Highly Strained InAs/GaAs Monolayer

S. Reich[1]), A. R. Goñi, C. Thomsen, F. Heinrichsdorff, A. Krost,
and D. Bimberg

*Institut für Festkörperphysik, Technische Universität Berlin, PN 5-4, Hardenbergstr. 36, D-10623 Berlin, Germany*

Using Raman spectroscopy we studied the InAs-related vibrations of a single highly strained InAs monolayer embedded in bulk-like GaAs. Experiments were performed in right-angle and forward-scattering configuration with the scattered light propagating along the monolayer plane. The energies of the InAs modes are strongly blue-shifted compared to the bulk values. We estimate the phonon deformation potentials of InAs and obtained the strain in the monolayer to be $-5\%$.

Highly strained low-dimensional structures exhibit fascinating properties resulting from the combination of the effects of confinement and biaxial strain. Confinement manifests itself in the formation of discrete electronic and vibrational states. In the zero-dimensional limit, these structures, i.e., quantum dots, have atomic-like spectra although they consist of thousands of atoms [1]. In addition, a biaxial strain in III–V semiconductors lifts the cubic symmetry of the unit cell. The triply degenerate optical phonons of the bulk crystal split into a strain-induced doublet and singlet component vibrating parallel and perpendicular to the strain direction, respectively. The study of vibrations in lattice-mismatched heterostructures can provide insight into the strain present in the system. This information is essential for a deeper understanding of the optical and electronic properties of the low-dimensional structures.

In many ways, vibrations in quantum wells can be related to those in the more extensively studied superlattices [2 to 4], one major difference being the symmetry. Since a translational symmetry in the growth direction is missing in quantum wells, they belong to the $D_{2d}$ or $C_{2v}$ point group, depending on whether the number of monolayers in the well is even or odd, respectively. An effect of the $C_{2v}$ point group, in particular, is that the $x$- and $y$-axis − now being parallel to the [110] and [1$\bar{1}$0] direction of the bulk crystal − are no longer related by symmetry. The orthorhombic distortion of odd-number monolayers is, however, expected to be small because of the surrounding higher-symmetry bulk.

In this paper we report on Raman scattering in a single highly strained InAs monolayer embedded in bulk-like GaAs. We performed experiments in right-angle and forward-scattering configuration with the scattered light propagating along the layer plane (Fig. 1). This allowed us the observation of phonons with various propagation direc-

---

[1]) Corresponding author: Tel.: +49-30-314-23468; Fax: +49-30-314-27705;
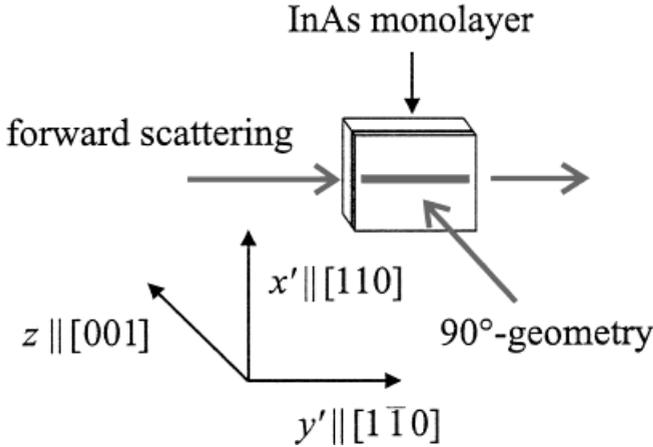e-mail: steffi@physik.tu-berlin.de

Fig. 1. Scattering geometries used; the growth direction of the sample was [001]

tions in contrast to standard backscattering along the growth direction. We find that the phonon modes of the InAs monolayer are blue-shifted compared to unstrained bulk InAs and show significant angular dispersion. By assuming that the highest (lowest) frequency in the energy range of the InAs optical modes corresponds to the strain-induced singlet (doublet) component we estimate the phonon deformation potentials of InAs and the built-in strain of the monolayer.

The sample was grown by metalorganic vapor phase deposition on a semiinsulating (001) GaAs substrate as described elsewhere [5]. The InAs layer with an effective thickness of 1.5 monolayers (ML) is surrounded by 600 nm bulk-like GaAs. The band gap of the structure is known from luminescence measurements to be 871 nm; details about the optical properties can be found in Ref. [6]. The single InAs/GaAs layer was sandwiched between two cladding layers of undoped $Al_{0.5}Ga_{0.5}As$ forming a waveguide. Raman spectra were excited at low temperature (6 K) using a tunable Ti-sapphire in the range 868 to 880 nm, in resonance with the fundamental gap of the monolayer and below. The scattered light was analyzed with a DILOR XY 800 spectrometer in combination with a charge coupled device (CCD) detector. The scattering geometries and the coordinate system used in this paper are indicated in Fig. 1. The selection rules for Raman-scattering in crystals belonging to the $D_{2d}$ and $C_{2v}$ point group are summarized in Table 1. Note that

Table 1

Raman-scattering selection rules for the $D_{2d}$ and $C_{2v}$ point group. In the $D_{2d}$ point group $z$-polarized modes belong to the $B_2(z)$ and $A_1$ representations depending on the confinement index [2,3], while $x'$- and $y'$-polarized modes have $E(x')$ and $E(y')$ Raman tensor. Note the correlation of the $D_{2d}$ to the $C_{2v}$ point group: The $B_2(z)$ and $A_1$ representions are correlated to $A_1$, while the E representation corresponds to $B_1 + B_2$ [14]

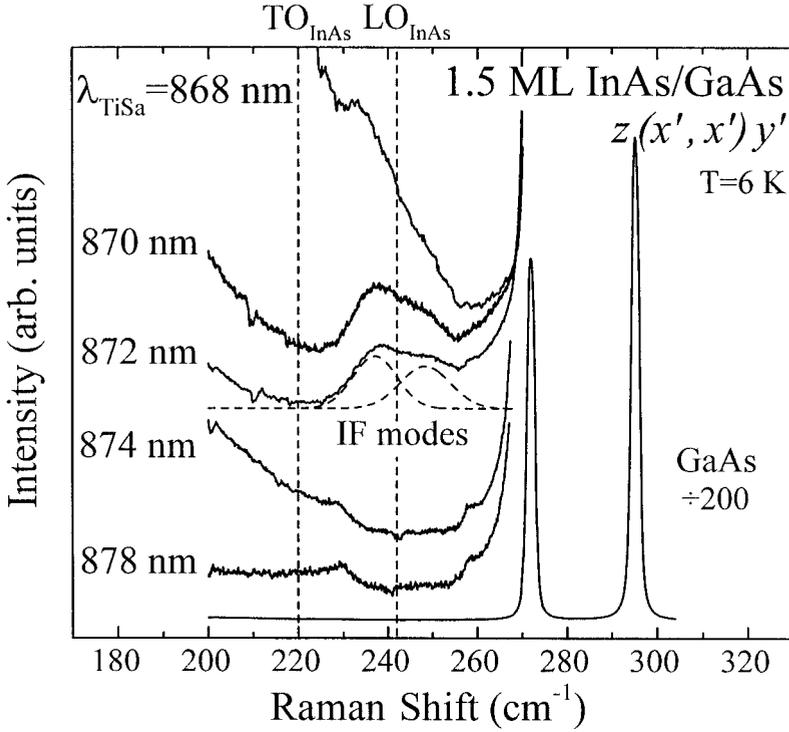| right-angle geometry | | | forward scattering | | |
|---|---|---|---|---|---|
| | $D_{2d}$ | $C_{2v}$ | | $D_{2d}$ | $C_{2v}$ |
| $z(x', x')y'$ | $B_2(z)$, $A_1$ | $A_1$ | $y'(x', x')y'$ | $B_2(z)$, $A_1$ | $A_1$ |
| $z(x', z)y'$ | $E(x')$ | $B_1$ | $y'(x', z)y'$ | $E(x')$ | $B_1$ |
| $z(y', x')y'$ | – | – | $y'(z, z)y'$ | $A_1$ | $A_1$ |
| $z(y', z)y'$ | $E(y')$ | $B_2$ | | | |

Fig. 2. Raman spectra in right-angle $z\,(x',\,x')\,y'$ geometry at different excitation wavelengths. The spectra at 868 to 872 nm correspond to resonant, at 874 and 878 nm to non-resonant conditions. For the spectra at 872 nm a fit to the IF modes is shown (dashed curves). The vertical lines indicate the frequencies of the unstrained bulk InAs TO and LO phonons. The spectra are shifted for clarity

the symmetry of a given mode depends on its polarization direction, which, in general, is mixed for wave vectors lying not parallel to the $z$-axis.

Fig. 2 shows Raman spectra taken in right-angle geometry at different excitation wavelengths. The two strong peaks at 273 and 296 cm$^{-1}$ are the GaAs TO and LO phonons, respectively. The GaAs modes are neither shifted nor broadened compared to the bulk. Below 270 cm$^{-1}$ we observe structures 200 times weaker in intensity which are due to scattering by InAs phonons. As indicated in the figure, the InAs related modes are blue-shifted compared to the bulk values (dashed vertical lines) due to the huge built-in strain $\varepsilon = (a_{GaAs} - a_{InAs})/a_{InAs} = -6.7\%$. We estimated the LO (TO) frequency range to be 245 to 265 cm$^{-1}$ (230 to 240 cm$^{-1}$) by taking into account the hydrostatic component of the biaxial strain and adding a typical shear-strain splitting [2,7] in III–V semiconductors. The spectral line shape in this region strongly depends on the wavelength of the exciting laser. Under resonant excitation we found two broad peaks centered at 237 cm$^{-1}$ and 247 cm$^{-1}$ (dashed curves), which disappear for laser energies below the fundamental gap of the InAs/GaAs structure. We ascribe them to scattering by interface (IF) modes. It was shown by Shields et al. [8] that in two-dimensional systems Raman spectra are dominated by interface modes under resonance conditions. They described this as a fourth-order process induced by elastic scattering and Fröhlich interaction. Con-

sequently, Raman scattering should be allowed in parallel but forbidden in crossed polarization. However, a signal of one half the intensity is commonly found in crossed polarization as well [8]. When changing the excitation energy from resonant (upper traces in Fig. 2) to non-resonant (lower traces) the interface modes decrease rapidly in intensity, whereas two distinct peaks become apparent at 230 and 259 cm$^{-1}$. They also seem to be present in resonant spectra (see the feature at 259 cm$^{-1}$ in the spectrum at $\lambda_{TiSa} = 872$ nm). These modes have no angular dispersion because we observed them in backscattering $y'(\,.\,.\,)\overline{y'}$ along the layer plane, too. We tentatively assign the lower mode (230 cm$^{-1}$) to a confined TO-like vibration. The selection rules are, however, not completely consistent with this assignment as the TO mode appears only in parallel polarization both in right-angle and forward-scattering (see Fig. 3) configuration.

In forward scattering (see Fig. 3) the spectra exhibit strikingly strong features in the energy range where the LO phonons of the InAs monolayer are expected. Between 240 and 265 cm$^{-1}$ the spectra resemble a phonon density of states. One can clearly see one peak at 264 cm$^{-1}$ indicating probably flat dispersion and a less pronounced one around 255 cm$^{-1}$ with a sharp cut-off at 240 cm$^{-1}$. In the TO frequency range we find a weak peak at 229 cm$^{-1}$, which is only seen in parallel polarization. This peak looks like the one found in right-angle geometry out of resonance. Probably, the spectral shape between 240 and 265 cm$^{-1}$ reflects the angular dispersion of the LO-like confined modes of the InAs monolayer. Since the phonon wave vector is perpendicular to that of the light in forward-scattering experiments, all modes with a wave vector in a plane perpendicular to $y'$ can scatter. The interpretation as an angular density of states, however, raises a problem.
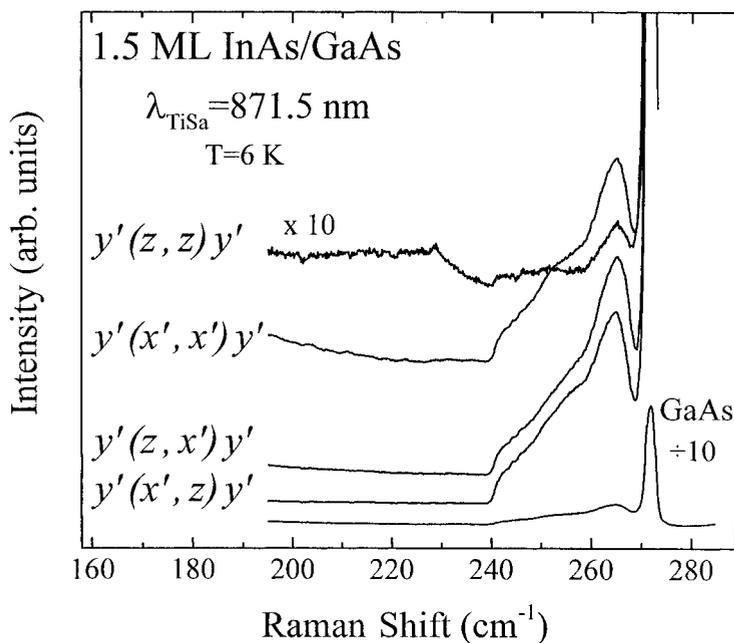


Fig. 3. Raman spectra at 871.5 nm excitation wavelength in different forward-scattering configurations. The spectrum in $y'(z, z)y'$ was multiplied by ten

The angular phonon dispersion [2, 3, 9] in quantum wells and superlattices arises from the electrostatic field produced by a vibration in a polar material. In the limit of the quantum-well thickness tending to zero there is no frequency shift when the wave vector $\mathbf{q}$ is rotated from the growth direction to a direction in the layer plane (usually, this is expressed in terms of an angle $\Theta(\mathbf{q}, z)$ varying between $0°$ and $90°$). In this model the polarization direction is completely fixed and only the character of the mode changes from LO-like ($\Theta = 0°$) to TO-like ($\Theta = 90°$), and *vice versa* for the TO-like modes at $0°$. Since the polarization of the mode ends up fixed, one does not get any dispersion due to strain either. When adopting this confinement point of view there are no modes in the InAs monolayer originating from the strain induced LO doublet and TO singlet in a bulk crystal. On the other hand, there is the strain point of view [10]. This picture starts with a biaxially strained crystal and different frequencies for the modes vibrating parallel and perpendicular to the strain. If confinement is included at all, it is added afterwards in the spirit of confined modes, i.e. by introducing a small frequency shift due to the quantization of $q_z$. This model, however, fails in the description of the electrostatic potential. Both pictures have their shortcomings and further work is needed to describe strain properly in the angular phonon dispersion.

Our measurements clearly do show some angular dispersion. For an estimate of the strain in the InAs monolayer and the shear deformation potentials we identified the peak at the highest frequency (264 cm$^{-1}$) with the singlet component LO$_s$ and the interface mode (247 cm$^{-1}$) with the doublet component LO$_d$, and similarly for the TO singlet 237 cm$^{-1}$ and the TO doublet 229 cm$^{-1}$. The strain $\varepsilon$ and the shear deformation potentials [10, 11] are given by

$$\varepsilon = -\frac{1}{\omega_0} \frac{(3\omega_0 - \Omega_s - 2\Omega_d)}{(\tilde{K}_{11} + 2\tilde{K}_{12})(1 - C_{12}/C_{11})} , \tag{1}$$

$$(\tilde{K}_{11} - \tilde{K}_{12}) = \frac{2(\Omega_s - \Omega_d)(\tilde{K}_{11} + 2\tilde{K}_{12})}{(3\omega_0 - \Omega_s - 2\Omega_d)} \frac{(1 - C_{12}/C_{11})}{(1 + 2C_{12}/C_{11})}, \tag{2}$$

where $\omega_0$ is the strain-free frequency, $\Omega_s$ and $\Omega_d$ are the frequencies of the singlet and the doublet components, respectively, $(\tilde{K}_{11} + 2\tilde{K}_{12}) = -6\gamma$ is the phonon deformation potential due to hydrostatic strain, and $C_{ij}$ are the elastic moduli. Both equations hold for LO and TO modes, the subscript being omitted for clarity. In $\omega_0(\text{LO})$ we included a small red-shift of 1 cm$^{-1}$ due to confinement. From (1) we obtain a strain $\varepsilon = -(4.9 \pm 0.9)\%$ (LO components) and $\varepsilon = -(5.0 \pm 1.1)\%$ (TO components). This is less than the expected value of $-6.7\%$ due to the lattice mismatch between InAs and GaAs. A relaxation of the InAs monolayer might take place through thickness fluctuations during the growth process or by a slight deformation of the surrounding GaAs. InAs layers are indeed known to have localized excitons [6], which is commonly explained by a varying layer thickness. We also note that the effective thickness of the 1.5 InAs monolayer studied here is very close to the critical layer thickness (2 ML) in InAs/GaAs systems.

The shear deformation potentials obtained from (2) are $(\tilde{K}_{11} - \tilde{K}_{12})_{\text{LO}} = (1.35 \pm 0.4)$ and $(\tilde{K}_{11} - \tilde{K}_{12})_{\text{TO}} = (0.74 \pm 0.4)$. They seem to be quite large compared to GaAs (0.3 for the TO), but are of the same order as, e.g., in InP (0.69). Usually the LO shear deformation potential is about twice as large as the TO value in III–V semiconductors [2,7], in good agreement with our measurements. The value reported by Cerdeira et al.

[11] for bulk InAs $(\tilde{K}_{11} - \tilde{K}_{12})_{\text{TO}} = 0.57$ was measured using Raman spectroscopy on uniaxially strained crystals, where the excitation was above the InAs band gap. As was shown later [12,13], the shear deformation potentials obtained in this way are too small (typically by 30%) due to surface relaxation, thus confirming again our larger values.

In conclusion, we have studied the vibrational properties of a single highly strained 1.5 InAs monolayer surrounded by bulk-like GaAs. We have presented Raman spectra in right-angle and forward-scattering in-plane geometries. From our measurements we obtained the InAs phonon deformation potentials and the strain in the monolayer.

## References

[1] C. WEISBUCH and B. VINTER, Quantum Semiconductor Structures: Fundamentals and Applications, Academic Press, San Diego (CA) 1991.
   D. BIMBERG, M. GRUNDMANN, and N. N. LEDENTSOV, Quantum Dot Heterostructures, John Wiley & Sons, New York 1999.
[2] B. JUSSERAND and M. CARDONA, in: Light Scattering in Solids V: Superlattices and Other Microstructures, Eds. M. CARDONA and G. GÜNTHERODT, Topics in Applied Physics, Vol. 66, Springer-Verlag, Berlin/Heidelberg/New York 1989 (p. 49).
[3] A. FAINSTEIN, P. ETCHEGOIN, M. P. CHAMBERLAIN, M. CARDONA, K. TÖTEMEYER, and K. EBERL, Phys. Rev. B **51**, 14448 (1995).
[4] M. SIAKAVELLAS, Y. S. RAPTIS, E. ANASTASSAKIS, and D. J. LOCKWOOK, J. Appl. Phys. **82**, 6235 (1997).
[5] A. KROST, F. HEINRICHSDORFF, D. BIMBERG, A. DARHUBER, and G. BAUER, Appl. Phys. Lett. **68**, 785 (1996).
[6] A. R. GOÑI, M. STROH, C. THOMSEN, F. HEINRICHSDORFF, V. TÜRCK, A. KROST, and D. BIMBERG, Appl. Phys. Lett. **72**, 1433 (1998).
   A. CANTARERO, A. R. GOÑI, S. REICH, C. THOMSEN, and P. V. SANTOS, in preparation.
[7] F. POLLACK, in: Strained-Layer Superlattices: Physics, Semiconductors and Semimetals, Vol. 32, Ed. T. PEARSALL, Academic Press, New York 1990 (p. 19).
[8] A. J. SHIELDS, M. CARDONA, and K. EBERL, Phys. Rev. Lett. **72**, 412 (1994).
   A. J. SHIELDS, M. P. CHAMBERLAIN, M. CARDONA, and K. EBERL, Phys. Rev. B **51**, 17728 (1995).
[9] M. ZUNKE, R. SCHORER, G. ABSTREITER, W. KLEIN, and G. WEIMANN, Solid State Commun. **93**, 847 (1995).
[10] E. ANSTASSAKIS, J. Appl. Phys. **81**, 3046 (1996).
[11] F. CERDEIRA, C. J. BUCHENAUER, F. H. POLLACK, and M. CARDONA, Phys. Rev. B **5**, 580 (1972).
[12] P. WICKBOLDT, E. ANASTASSAKIS, R. SAUER, and M. CARDONA, Phys. Rev. B **35**, 1362 (1987).
[13] E. ANASTASSAKIS, Y. RAPTIS, M. HÜNERMANN, W. RICHTER, and M. CARDONA, Phys. Rev. B **38**, 7702 (1988).
[14] D. L. ROUSSEAU, R. P. BAUMAN, and P. S. PORTO, J. Raman Spectroscopy **10**, 252 (1981).